Int. J. Heat Mass Transfer. Vol. 23, pp. 1091–1097.

0017-9310/80/0801-1091 $02.00/0

HEAT TRANSFER BY A FREE CONVECTION LOOP EMBEDDED IN A HEAT-CONDUCTING SOLID

K. E. TORRANCE and V. W. C. CHAN
Sibley School of Mechanical and Aerospace Engineering,
Cornell University, Ithaca, New York 14853, U.S.A.

(*Received* 10 *September* 1979 *and in revised form* 8 *January* 1980)

Abstract — An open, free convection loop embedded near the surface of a heat-conducting solid is examined numerically. The loop is in the form of a half-torous with duct diameter d and toroidal major radius $D/2$. The solid is heated uniformly from below. Critical Rayleigh numbers (Ra_c) for the onset of motion are determined. Velocities, exit temperatures, and convective heat transfer rates are determined for d/D values of 10^{-2}, 10^{-3} and 10^{-4} and for Rayleigh number ratios (Ra/Ra_c) from 1 to 360. The Prandtl number is 2.8 and the fluid/solid thermal conductivity ratio is $k_f/k_s = 0.133$. Results are compared with an analytical solution [7] for a high-conductivity solid, i.e. $k_f/k_s \to 0$.

NOMENCLATURE

c, constant of order unity;
c_{pf}, specific heat of fluid;
d, duct diameter;
D, toroidal major diameter;
f, friction factor;
g, acceleration of gravity;
h_c, heat-transfer coefficient;
k_f, thermal conductivity of fluid;
k_s, thermal conductivity of solid surrounding the loop;
$\bar{u}$, mean fluid velocity;
Nu, Nusselt number defined in equation (9);
Pr, Prandtl number of fluid defined in equation (9);
Q_c, convective heat flow from loop defined by equation (16);
Q_∞, conductive heat flow at depth across area D^2, defined by equation (17);
Q', heat flow per unit length of loop;
Q'_i, heat flow per unit length of image loop;
r, s, z, distance from centerline of loop to any point P in the solid, axial coordinate along loop, and vertical depth, all defined in Fig. 1;
R, S, Z, dimensionless distance from centerline of loop to any point in the solid, dimensionless axial coordinate, and dimensionless vertical depth;
Re, Reynolds number defined in equation (9);
Ra, Rayleigh number defined in equation (9);
Ra_c, critical Rayleigh number for the onset of convective flow;
Ra_c^*, critical Rayleigh number for a loop surrounded by a high-conductivity solid, defined in equation (15);
T_b, fluid bulk temperature;
T_{bi}, T_{be}, inlet and exit fluid bulk temperatures;
T_0, constant surface temperature shown in Fig. 1;
$\overline{T_w}$, mean wall temperature;
$(\partial T/\partial z)_\infty$, ambient temperature gradient far from the loop.

Greek symbols

α_f, thermal diffusivity of fluid;
β_f, thermal expansion coefficient of fluid;
ΔT, reference temperature difference, $(\partial T/\partial z)_\infty D/2$;
θ, dimensionless temperature, $(T - T_0)/\Delta T$;
$\theta_b, \theta_{bi}, \theta_{be}$, dimensionless bulk, inlet bulk, and exit bulk temperatures;
$\overline{\theta_w}$, dimensionless mean wall temperature;
ρ_f, density of fluid;
ϕ, angular coordinate shown in Fig. 1;
ν_f, kinematic viscosity of fluid.

INTRODUCTION

THIS PAPER examines an open, free convection loop embedded near the surface of a heat-conducting solid. The loop is in the form of a half-torous as shown in Fig. 1. Although idealized, the geometry is representative of fluid-filled pores at an interface between a heated permeable medium and a cooling fluid. The geometry is also representative of aquifers embedded in geological formations. Under appropriate conditions, heat

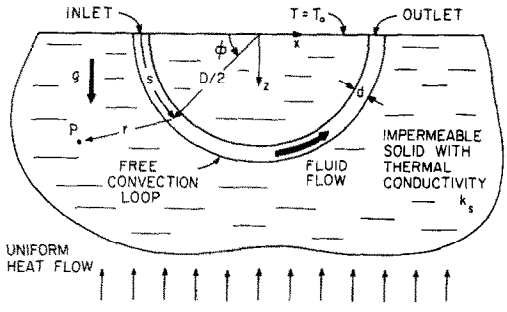

FIG. 1. Illustration of open-loop geometry.

conduction through the surrounding solid will establish a natural circulation through the loop. This flow will, in turn, augment the transfer of heat from the interior of the solid to its surface. Clearly, the process of heat conduction in the solid interacts with, and is altered by, the natural convection flow through the open loop. This combined conduction–convection problem forms the subject of the present paper.

Natural circulation loops, also known as loop thermosyphons, have been widely studied in the engineering literature. Indeed, thermosyphons have been the subject of a review by Japikse [1]. Most prior studies have examined closed loops where the wall temperature or wall heat flux was a known function of position. This includes experimental and theoretical studies of toroidal [2, 3] and straight-segment [4, 5] loops. Relatively few studies have been made of open loop systems, however. An open loop is one which connects points of inflow and outflow, each of which is maintained at a known pressure. Open-loop thermosyphons have been examined in the engineering [6] and geophysical [7] literature. Indeed, in the latter area, approximate models have been constructed to simulate the conductive resistance of surrounding rock formations. However, the heating of the thermosyphon was either prescribed [8] or attributed to transient conduction from the surroundings [9]. It appears that problems involving combined conduction–convection at steady state between a free convection loop and its surroundings have not been considered.

This work considers the free convection loop sketched in Fig. 1. The loop is a circular duct (of diameter d) whose centerline describes a semi-circle (of radius $D/2$). The resulting half-torous is embedded in an otherwise-impermeable solid of uniform thermal conductivity k_s. The loop is filled with fluid of thermal conductivity k_f. Inflow and outflow to the loop occur on a horizontal, isothermal boundary of the solid. The solid is heated uniformly at depth where a uniform temperature gradient $(\partial T/\partial z)_\infty$ exists. Any free convection through the loop alters this gradient in the immediate vicinity of the loop. The natural circulation is, of course, driven by density differences between the descending and ascending legs of the loop.

An analytical model for steady state, combined conduction–convection in the loop is proposed in the following section. The model employs integrated, one-dimensional balances of heat and momentum within the loop, and uses distributed sources and sinks of heat to solve the external conduction equation. A Prandtl number characteristic of water and a k_f/k_s ratio typical of water and an intermediate-conductivity solid are assumed. Numerical solutions are obtained which include a determination of the critical Rayleigh number, Ra_c, for the onset of convective flow. The flow rate through the loop, expressed by the product $RePrd/D$, is found for a range of Rayleigh numbers and for several values of d/D. Laminar, transitional, and turbulent flows are considered. Exit temperatures and rates of convective heat transfer are also determined. Results are compared with an analysis applicable to a high-conductivity solid.

FORMULATION

Consider the loop illustrated in Fig. 1. Following prior work [7], area- averaged momentum and energy balances may be written for steady flow conditions as

$$-\rho_f g\beta_f c\int_0^{\pi D/2}(T_b - T_0)\cos\phi\,\mathrm{d}s = \frac{\pi}{4} f\rho_f \bar{u}^2 \frac{D}{d} \quad (1)$$

$$\frac{\rho_f c_{pf} d}{4}\bar{u}\frac{\mathrm{d}T_b}{\mathrm{d}s} = -h_c(T_b - \bar{T}_w) \quad (2)$$

where $\bar{u}$ is the mean velocity (a constant), $T_b(s)$ and $\bar{T}_w(s)$ are respectively the fluid bulk temperature and the mean wall temperature at any axial station, and f and h_c are the friction factor and heat-transfer coefficient for pipe flow. Other parameters are defined in the Nomenclature list.

In equation (1), the left and right sides respectively represent the net buoyant head and the friction head. In general, an elevation difference h between inlet and outlet could be included by adding a term $\rho_f gh$ to the left side, but such topographic effects will not be considered in the present study. The coefficient c is the ratio of the area-mean fluid temperature (which characterizes the buoyant force) to the bulk or mixed-mean fluid temperature (which describes convective energy flow). The coefficient depends on the cross-sectional profiles of velocity and temperature in the duct. The value of c ranges from slightly less than unity (turbulent flow) to approximately 8/11 (laminar flow). Due to the approximate nature of the present analysis a value of $c = 1$ is justified for most applications.

In the energy equation (2) note that axial conduction, viscous dissipation, and a term involving the adiabatic temperature gradient have been neglected. The latter two effects are proportional to a parameter known as the dissipation number [10], $Di = \beta_f gD/2c_{pf}$. The two effects have been included for laminar flows in the present geometry [11] and were found to be of the same order and generally small for most applications. In general, viscous dissipation and the adiabatic temperature gradient may be neglected in natural convection problems when the dissipation number is small compared to unity.

The temperature in the solid surrounding the free convection loop is governed by Laplace's equation. An appropriate solution for the temperature at any point P can be obtained by the superposition of point sources and point sinks of heat along the centerline of the loop [12]. To satisfy the surface boundary condition it is necessary to introduce a mirror-image loop, embedded in a heat-conducting solid, above $z = 0$. The axial coordinate s is extended to the image loop (over the range $\pi D/2 \le s \le \pi D$). The heat flow to the surrounding solid from the true or image loops, per unit length along the loops, is denoted by Q' or Q'_i, respectively. Any heat released by the true loop must

be absorbed by the image loop. The isothermal boundary condition at $z = 0$ is satisfied by requiring that $Q_i'(\pi D - s) = -Q'(s)$ over the range $0 < s < \pi D/2$ (discontinuities may exist at $s = 0$ and $\pi D/2$). The temperature at any point P in the surrounding solid is thus given by

$$T(x, y, z) = \int_0^{\pi D/2} \frac{Q'(s)\mathrm{d}s}{4\pi k_s r} + \int_{\pi D/2}^{\pi D} \frac{Q_i'(s)\mathrm{d}s}{4\pi k_s r} + T_0 + \left(\frac{\partial T}{\partial z}\right)_\infty z \quad (3)$$

where T_0 is the surface temperature (at $z = 0$), $(\partial T/\partial z)_\infty$ denotes the uniform heat flux into the solid from below, and the integrals of heat loss from the actual and image loops appear on the right side.

The mean wall temperature $\overline{T_w}(s)$ is found by averaging the temperature given by (3) around the circumference of the duct at any axial station. The source–sink distribution is then eliminated from the averaged equation by using the identity

$$Q'(s) = \pi h_c \mathrm{d}(T_b - \overline{T_w}). \quad (4)$$

The result is

$$\overline{T_w}(s) = \frac{h_c d}{4k_s}\int_0^{\pi D} (T_b - \overline{T_w})\frac{\mathrm{d}s}{r} + T_0 + \left(\frac{\partial T}{\partial z}\right)_\infty z \quad (5)$$

where temperatures in the image loop are suitably interpreted. Equation (5) is a weakly-singular, non-homogeneous Fredholm integral equation of the second kind.

The governing equation may be cast in parametric form by introducing dimensionless variables. Appropriate reference quantities are, for a length scale, the depth (or radius) of the loop, $D/2$, and, for a temperature scale, the temperature difference between the bottom of the loop and the surface of the solid, $\Delta T = (\partial T/\partial z)_\infty D/2$. The governing equations (1), (2) and (5) thus become

$$-\int_0^\pi \theta_b \cos\phi \,\mathrm{d}S = \pi f \frac{Re^2 Pr}{Ra}\frac{d}{D} \quad (6)$$

$$\frac{\mathrm{d}\theta_b}{\mathrm{d}S} = -2\frac{Nu}{RePr}\frac{D}{d}(\theta_b - \overline{\theta_w}) \quad (7)$$

$$\overline{\theta_w} = \frac{1}{4}Nu\frac{k_f}{k_s}\int_0^{2\pi}(\theta_b - \overline{\theta_w})\frac{\mathrm{d}S}{R} + Z \quad (8)$$

where S, R and Z are dimensionless lengths and $\theta = (T - T_0)/\Delta T$. The parameters which appear are identified as Reynolds, Prandtl, Rayleigh and Nusselt numbers

$$Re = \frac{\bar{u}d}{\nu_f}, \quad Pr = \frac{\nu_f}{\alpha_f}, \quad Ra = \frac{g\beta_f c(\partial T/\partial z)_\infty d^4}{\nu_f \alpha_f}, \quad Nu = \frac{h_c d}{k_f}. \quad (9)$$

To complete the problem formulation, forced convection correlations for the friction factor and Nusselt number are assumed. These are [12, 13]:

$$f = 64/Re, \quad Nu = 48/11 \quad (10)$$

for laminar flow ($Re < 2300$) and

$$f = 0.316\,Re^{-0.25}, \quad Nu = 0.023\,Re^{0.8}Pr^{1/3} \quad (11)$$

for turbulent flow ($Re > 3300$). Linear interpolation is used for the transitional regime ($2300 \le Re \le 3300$). The Nusselt number given in (10) applies for constant-flux wall heating; the Nusselt number given in (11) applies for both constant-flux and constant-wall-temperature heating conditions. The foregoing correlations should provide reasonable estimates whenever secondary flows due to curvature or mixed convection are small [12, 14]. Thus, although the mean flow is driven by density differences between ascending and descending legs of the loop, secondary flows (and density differences) at any axial station are neglected.

The usual unknowns in the present problem are the mean velocity, $\bar{u}$, and the bulk and wall temperature distributions in the loop. In dimensionless form, these unknowns appear in the Reynolds number, Re, and the temperature distributions $\theta_b(S)$ and $\overline{\theta_w}(S)$. These unknowns are governed by equations (6) to (8), with f and Nu given by (10) and (11). The governing equations form a set of nonlinear (in Re), coupled, differential and integral equations. In general, solutions must be obtained numerically. One boundary condition appears in the governing equations: the inlet fluid temperature θ_{bi}. We will assume that fluid enters at the surface temperature so that $\theta_{bi} = 0$. The independent parameters of the problem thus become Pr, Ra, d/D, and k_f/k_s.

NUMERICAL SOLUTIONS

A principal goal of the study is to find the flow rate, the outflow temperature, and the convective heat transport from a syphon when all other parameters are given. Since the governing equations are nonlinear in Re, they are not readily solved for this variable. Instead, solutions were found by assuming a value for Re and then finding the value of Ra required to balance the flow.

A solution proceeds by assuming Re and solving (7) and (8) for the temperature distributions, θ_b and $\overline{\theta_w}$, along the loop. Finite differences were used. A backward difference was employed (for stability reasons) for the spatial derivative in (7). The mean wall temperature, $\overline{\theta_w}(s)$, was found by averaging, at each axial station, the temperature given by (3) at four equally-spaced points around the circumference of the duct. Trapezoidal-rule integration was then used for (8). Although a direct algebraic solution for θ_b and $\overline{\theta_w}$ at discrete points is possible in principle, the number of unknowns is generally too large to handle with accuracy. Instead, in practice a two-step iteration was found to be effective. First, θ_b was found from (7) using an estimate of $\overline{\theta_w}$. Second, the $\overline{\theta_w}$ estimate was improved by solving (8) using the new θ_b-values. The

two-step process was repeated until convergence was achieved (typically within 10 iterations). In the second step, for small values of the coefficient of the integral in (8), successive substitution was successful for solving (8). For large values of the coefficient, a direct algebraic solution was required. In addition, for small values of d/D, a local analytical integration of (8) was used to accurately handle the logarithmic singularity. Spatial step sizes of $\Delta S = 0.01\,\pi$ and $0.025\,\pi$ were used for the successive substitution and direct procedures, respectively.

After the temperature distributions were obtained, the integral in (6) was evaluated using trapezoidal-rule integration. The Ra-value required to balance the flow was obtained from (6). Solutions were obtained in this way for a range of Re. Additional details are available in reference [11].

RESULTS

Numerical solutions have been carried out to obtain flow rates and heat transfer characteristics for the free convection loop, or thermosyphon, shown in Fig. 1. Results are presented for a wide range of Rayleigh numbers and d/D ratios. A Prandtl number of $Pr = 2.8$ is assumed (water at 65°C). This choice of Pr does not influence the laminar flow solutions, however. A thermal conductivity ratio for the fluid and surrounding solid of $k_f/k_s = 0.133$ is assumed. For water as the fluid, this corresponds to a thermal conductivity for the solid which is intermediate between metals and nonmetals.

In what follows, it will be convenient to compare the numerical solutions with an analytical solution from reference [7]. The analytical solution assumes that the solid surrounding the loop has a very high thermal conductivity so that the ratio $k_f/k_s \to 0$. In this limit, the integral in (8) may be neglected and the wall temperature along the loop becomes a known function of depth (or position), i.e. $\bar{\theta}_w = Z$. The energy and momentum equations, (7) and (6), may be integrated to respectively obtain the bulk temperature distribution along the loop

$$\theta_b = \frac{N}{1+N^2}\left[e^{-SN} + \frac{1}{N}\sin S - \cos S\right] \quad (12)$$

and an equality between buoyant and friction heads,

$$\frac{\pi/2}{1+N^2} - \frac{N}{(1+N^2)^2}(e^{-\pi N} + 1) = 2\pi f \frac{ReNu}{Ra} \quad (13)$$

where

$$N = \frac{1}{2}\frac{RePr}{Nu}\frac{d}{D}. \quad (14)$$

The analytical solution also reveals the existence of a critical Rayleigh number for the onset of convection through a free convection loop. The critical Rayleigh number may be found from (13) by letting $N \to 0$. Denoting the critical Ra from the analytical solution by Ra_c^*, the result is $Ra_c^* = 4fReNu$. Since laminar flows are expected at the onset of motion, f and Nu may be evaluated with (10) to obtain

$$Ra_c^* = 12\,288/11 = 1117.1. \quad (15)$$

The critical Rayleigh number for the onset of convection in the loop is completely analogous to a critical Rayleigh number for the onset of motion in a fluid layer heated from below [12]. For both the loop and the layer, thermal and viscous damping suppress fluid motion when Ra is less than the critical value. When Ra is greater than the critical, buoyancy forces accelerate the flow until a balance exists between buoyancy and frictional forces. For the free convection loop, the thermal and viscous damping are respectively provided by wall heat transfer and by wall friction. The wall heat transfer rate is, in turn, influenced by the thermal conductivity of the solid surrounding the loop.

Numerically-determined critical Rayleigh numbers, Ra_c, are given in Fig. 2 for several d/D ratios and for the assumed thermal conductivity ratio of $k_f/k_s = 0.133$. The ordinate is scaled by the critical Rayleigh number for a loop embedded in a high-conductivity solid, Ra_c^* (equation (15)). Clearly, the critical Rayleigh numbers for the case $k_f/k_s = 0.133$ are less than Ra_c^*. This is readily understood if one examines the onset of convection in terms of a departure from a quiescent rest state. When the surrounding solid has a low thermal conductivity, any slight motion of fluid through the loop can alter the wall temperature along the loop. Thus, the local wall temperature is increased by ascending hot fluid, and is decreased by descending cold fluid. Such changes alter the buoyancy forces in a direction which helps to sustain fluid motion. The resulting critical Rayleigh number is therefore less than for a loop embedded in a high conductivity solid. For that case the flow of fluid does not alter the wall temperature to create a horizontal temperature difference to help sustain the flow.

Performance characteristics of the free convection loop are illustrated in Figs. 3, 4 and 5. These figures respectively display the flow rate, expressed as $RePr\,d/D$, the outlet temperature, θ_{be}, and the rate of heat convection out of the loop. The abscissa in all cases is the ratio Ra/Ra_c. The dotted lines in Figs. 3 and 4 represent the analytical solution expressed by (13) and (12), respectively, and were evaluated assuming laminar flow. The analytical solution corresponds to a loop embedded in a high-conductivity solid, i.e. $k_f/k_s \approx 0$. Solid and dashed lines correspond to numerically-obtained solutions for a conductivity ratio of $k_f/k_s = 0.133$. Results are shown for $d/D = 10^{-2}$,

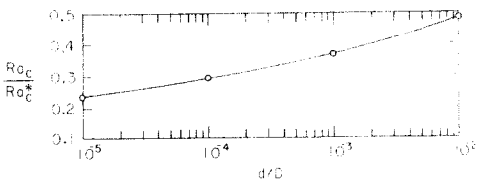

FIG. 2. Critical Rayleigh number vs. d/D for $k_f/k_s = 0.133$

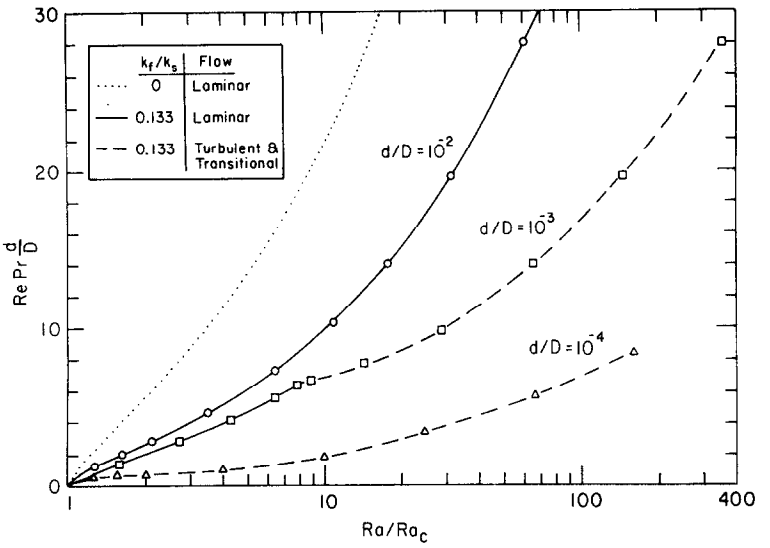

FIG. 3. Variation of mean velocity, expressed by the group $Re\ Pr\ d/D$, with Rayleigh number. The dotted line is from equation (13).

10^{-3} and 10^{-4}. Solid lines correspond to laminar flows, and dashed lines to transitional and turbulent flows.

Major features of the results will now be summarized. For laminar flows, with f and Nu given by (10), the governing equations (6) to (8) reveal that the unknown Reynolds number appears only in the group $Re\ Pr\ d/D$. Figure 3 illustrates this group. From Fig. 3, it is apparent for a given value of Ra/Ra_c that laminar flow rates are reduced by about 50 per cent when a finite-conductivity solid (with $k_f/k_s = 0.133$) is considered. Flow rates are further reduced by the transition to turbulence due to increased friction losses.

Outlet temperatures shown in Fig. 4 reveal a striking similarity of the laminar results for $k_f/k_s = 0$ and 0.133. Maximum outlet temperatures of 0.528 and 0.472 are observed for the two cases, and occur at Ra/Ra_c values of 3.5 and 4.3 respectively. Although the maximum achievable outflow temperatures are similar, the actual flow rates corresponding to the peaks are half as great for the case $k_f/k_s = 0.133$. The appearance of a peak outlet temperature at an intermediate value of Ra is discussed further in reference [7]. At low flow rates θ_b equilibrates to the wall temperature and the outflow temperature approaches the surface temperature, i.e. $\theta_{be} \to 0$. For very high flow rates the fluid in the loop

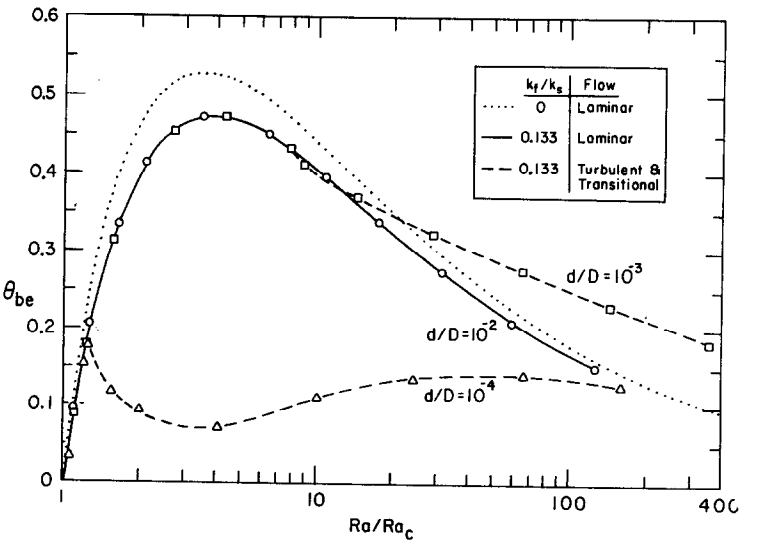

FIG. 4. Variation of outlet bulk temperature with Rayleigh number. The dotted line represents equation (12) evaluated at $S = \pi$.

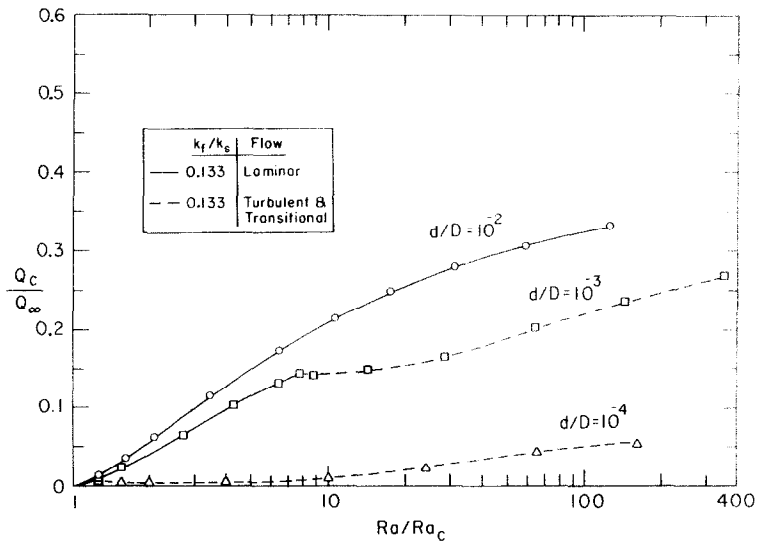

FIG. 5. Ratio of the convective heat flow (Q_c) to the ambient heat flow (Q_α) vs. Rayleigh number.

does not have time to be heated and in this limit $\theta_b \to 0$. Thus, a maximum outflow temperature occurs at an intermediate flow rate. Note also in Fig. 4 that the transition to turbulence can decrease or increase the outlet temperature for the case $k_f/k_s = 0.133$ depending upon whether Ra/Ra_c is less than or greater than 4.3. This is a direct consequence of the aforementioned change in the bulk temperature profiles with increasing flow rate. When $Ra/Ra_c < 4.3$ (low flow rates), θ_b near the exit is generally greater than θ_w. When $Ra/Ra_c > 4.3$ (high flow rates), the reverse is true just below the surface. Since the transition to turbulence tends to decrease the temperature difference $\theta_b - \bar{\theta}_w$, the result is the observed decrease or increase of θ_{be} accompanying the transition to turbulence.

An important aspect of the free convection loop is its ability to enhance the transfer of heat from the interior of the solid to its surface. This may be expressed by comparing the enthalpy difference between outlet and inlet of the loop

$$Q_c = (\pi d^2/4)\rho_f c_{pf} \bar{u}(T_{be} - T_{bi}) \tag{16}$$

with the conductive heat flow at depth. Quite arbitrarily, we select a reference area of size D^2 for the conductive heat flow

$$Q_\alpha = D^2 k_s (\partial T/\partial z)_\alpha. \tag{17}$$

The ratio of these two expressions is

$$\frac{Q_c}{Q_\alpha} = \frac{\pi}{8}\frac{k_f}{k_s} Re\, Pr \frac{d}{D}\theta_{be} \tag{18}$$

and is displayed in Fig. 5. An ordinate value near unity implies that the convective heat transfer by a loop is comparable to the heat conduction through an area D^2 at depth. Clearly, the ratio Q_c/Q_α increases as d/D is increased. This implies, if d is held constant, that shallow free convection loops are relatively more effective for transporting heat to the surface than are deep loops. Results in Fig. 5 also indicate that laminar flows are somewhat more effective for transporting heat than are turbulent flows; this follows from our prior discussion of the effects of turbulent transition on $Re\, Pr\, d/D$ and θ_{be} (Figs. 3 and 4). Thus, the rate of heat transfer would be increased if the transition to turbulence were delayed. From Fig. 5 we conclude that shallow free convection loops, employing laminar flow, provide the most effective means of enhancing the transfer of heat from the interior of the solid to its surface.

Acknowledgements — The authors would like to thank Professor Donald Turcotte for helpful discussions during the course of this work. This research has been supported by the Division of Engineering of the National Science Foundation under Grant ENG-7823542.

REFERENCES

1. D. Japikse, Advances in thermosyphon technology, *Advances in Heat Transfer*, edited by T. F. Irvine, Jr. and J. P. Hartnett, Vol. 9, pp. 1–11. Academic Press, New York (1973).
2. P. S. Damerell and R. J. Schoenhals, Flow in a toroidal thermosyphon with angular displacement of heated and cooled sections, *J. Heat Transfer* **101**, 672–676 (1979).
3. H. F. Creveling, J. F. de Paz, J. Y. Baladi and R. J. Schoenhals, Stability characteristics of a single-phase free convection loop, *J. Fluid Mech.* **67**, 65–84 (1975).
4. C. D. Alstad, H. S. Isbin, N. R. Amundson and J. P. Silvers, Transient behavior of single-phase natural-circulation loop systems, *A.I.Ch.E. Jl* **1**, 417–425 (1955).
5. Y. Zvirin and R. Grief, Transient behavior of natural circulation loops: two vertical branches with point heat source and sink, *Int. J. Heat Mass Transfer* **22**, 499–504 (1979).
6. J. L. Boy-Marcotte, P. Chevalier and M. Jannot, Study of temperature gradients due to gas thermosyphons induced within the Phenix nuclear reactor, *Heat Transfer and Turbulent Buoyant Convection*, edited by D. B. Spalding and N. Afgan, Vol. II, pp. 555–565. Hemisphere-McGraw-Hill, New York (1977).

7. K. E. Torrance, Open-loop thermosyphons with geological applications, *J. Heat Transfer* **101**, 677–683 (1979).
8. I. G. Donaldson, The simulation of geothermal systems with a simple convective model, *U.N. Symposium on the Development and Utilization of Geothermal Resources*, Pisa, *Geothermics* **2**(1), 649–654 (1970).
9. R. P. Lowell, Circulation in fractures, hot springs, and convective heat transport in mid-ocean ridge crests, *Geophys. J. R. Astronom. Sci.* **40**, 351–365 (1975).
10. D. L. Turcotte, A. T. Hsui, K. E. Torrance and G. Schubert, Influence of viscous dissipation on Bénard convection, *J. Fluid Mech.* **64**, 369–374 (1974).
11. Vincent W. C. Chan, A thermally driven fracture-flow model for warm springs, M.S. Thesis, Mechanical and Aerospace Engineering, Cornell University, Ithaca, New York (1978).
12. E. R. G. Eckert and R. M. Drake, Jr., *Analysis of Heat and Mass Transfer*, pp. 98–106, 340, 370, 536, 541–542. McGraw-Hill, New York (1972).
13. F. Kreith, *Principles of Heat Transfer*, 3rd edn, p. 445. Intext Press, New York (1973).
14. S. V. Patankar, V. S. Pratap and D. B. Spalding, Prediction of turbulent flow in curved pipes, *J. Fluid Mech.* **67**, 583–595 (1975).

TRANSFERT THERMIQUE ENTRE UNE BOUCLE A CONVECTION NATURELLE ET UN SOLIDE CONDUCTEUR DE LA CHALEUR

Résumé—Une boucle ouverte à convection naturelle près de la surface d'un silide conducteur de chaleur est examinée numériquement. La boucle est en forme de demi-tore avec un tube de diamètre d et un rayon $D/2$ du examinée numériquement. La boucle est en formetore. Le solide est chauffé uniformément par le bas. On détermine les nombres de Rayleigh critiques (Ra_c) pour l'apparition du mouvement. Des vitesses, des températures de sortie et des flux de transfert par convection sont déterminés pour des valeurs de d/D égales à 10^{-2}, 10^{-3} et 10^{-4} et pour des rapoorts (Ra/Ra_c) qui varient de 1 à 360. Le nombre de Prandtl est égal à 2,8 et le rapport des conductivités thermique du fluide et du solide est $k_f/k_s = 0{,}133$. Les résultats sont comparés avec une solution analytique [7] pour un solide à très haute conductivité, soit $k_f/k_s \to 0$.

WÄRMETRANSPORT DURCH FREIE KONVEKTION IN EINER SCHLAUFE, DIE IN EINEN WÄRMELEITENDEN FESTKÖRPER EINGEBETTET IST

Zusammenfassung—Eine nahe der Oberfläche eines wärmeleitenden Festköpers eingebettete offene Schlaufe wird bei freier Konvektion numerisch untersucht. Die Schlaufe hat die Form eines Halb-Torus mit dem Leitungsquerschnitt d und dem Torus-Hauptradius $D/2$. Der Festkörper wird gleichförmig von unten beheizt. Die kritische Rayleigh-Zahl Ra_c für das Einsetzen der Bewegung wird bestimmt. Geschwindigkeiten, Austrittstemperaturen und konvektive Wärmeübergangswerte werden für Werte d/D von 10^{-2}, 10^{-3} und 10^{-4} und Verhältnisse der Rayleigh-Zahlen (Ra/Ra_c) von 1 bis 360 bestimmt. Die Prandtl-Zahl ist 2.8 und das Verhältnis der Wärmeleitzahlen von Fluid und Festkörper ist $k_f/k_s = 0.133$. Die Ergebnisse werden verglichen mit einer analytischen Lösung [7] für einen hoch-wärmeleitenden Festkörper, d. h. $k_f/k_s \to 0$.

ТЕПЛОПЕРЕНОС СВОБОДНОЙ КОНВЕКЦИЕЙ В КОНТУРЕ, ВСТРОЕННОМ В ТЕПЛОПРОВОДНОЕ ТВЕРДОЕ ТЕЛО

Аннотация — Проведено численное исследование открытого контура у поверхности теплопроводного твердого тела, при этом в контуре имеет место свободная конвекция. Контур изготовлен в виде полутора с диаметром канала d и большим тороидальным радиусом $D/2$. Твердое тело равномерно нагревалось снизу. Определены значения критического числа Релея (Ra_c), соответствующие возникновению конвективного течения. Скорость, температура на выходе, а также скорость конвективного переноса тепла определялись при значениях d/D, равных 10^{-2}, 10^{-3} и 10^{-4} и при значениях отношения Ra/Ra_c в диапазоне от 1 до 360. Число Прандтля равнялось 2,8, а отношение теплопроводности жидкости к теплопроводности твердого тела составляло $k_f/k_s = 0{,}133$. Проведено сравнение результатов с аналитическим решением для случая высокотеплопроводного твердого тела, т. е. когда $k_f/k_s \to 0$.